



Computational thermodynamic analysis of compression ignition engine[☆]

A. Sakhrieh^a, E. Abu-Nada^{b,c,*}, I. Al-Hinti^c, A. Al-Ghandoor^d, B. Akash^e

^a Department of Mechanical Engineering, University of Jordan, Amman 11942, Jordan

^b Leibniz Universität Hannover, Institut für Technische Verbrennung, Welfengarten 1a, 30167 Hannover, Germany

^c Department of Mechanical Engineering, Hashemite University, Zarqa 13115, Jordan

^d Department of Industrial Engineering, Hashemite University, Zarqa 13115, Jordan

^e Department of Mechanical Engineering, King Faisal University, Al-Ahsa, 31982, Saudi Arabia

ARTICLE INFO

Available online 18 January 2010

Keywords:

Heat release modeling

Diesel cycle

Compression-ignition engine simulation

ABSTRACT

This paper presents diesel engine simulation taking into consideration heat transfer and variable specific heats. A dual Weibe function is used to model the heat release. It was found that early injection timing leads to higher levels of pressure and temperature in the cylinder. Also, it was found that BMEP is more sensitive to equivalence ratio than to engine speed. Higher values of equivalence ratio lead to lower thermal efficiency even an increase in the value of BMEP was revealed. For medium engine speeds between 2000 and 3000, it was found that the optimum equivalence ratio is between 0.5 and 0.7. However, for low engine speeds the optimum equivalence ratio was around 0.35. For high engine speeds the thermal efficiency was almost independent of equivalence ratios higher than 0.4.

© 2009 Elsevier Ltd. All rights reserved.

1. Introduction

Engine simulation has been used extensively in the last decades to improve engine performance [1–8]. Although air-standard power cycle analysis gives approximation to the actual conditions in real engines, it is very useful to compare the performance of air-standard power cycles using more reasonable assumptions (Pulkrabek, 2004). In recent studies carried out by the current authors, engine simulations were conducted taking into account the effect of heat loss, friction, rates of heat release, and temperature dependant specific heats on the overall engine performance [1–4]. The simulation code used in these studies employs a thoroughly validated thermodynamic, one-zone, zero-dimensional computational model.

Although the model was originally developed for spark ignition (SI) engines, it can be extended and modified to simulate compression ignition (CI) engines as well. The operation and performance analysis of CI engines and SI engines are very similar from a thermodynamic point of view, but the fundamental difference lies in the heat release model. While the combustion pattern in SI engines can be considered as totally premixed, both premixed and diffusion combustion coexist in CI engines. This results in a significant shift in the rate of heat release model from the simple Weibe function commonly used for SI engines. A double peak heat release model becomes more representative CI engines [9,10]. The first peak accounts for the heat release by

premixed combustion which is considered very rapid due to the vaporization of the fuel during the ignition delay period. The second peak occurs during heat release by the mixing controlled combustion which is considered as diffusion combustion. Different modified versions of this model have been reported in literature taking into account the effect of various parameters. For example, Arrègle et al. [11] studied the influence of injection parameters and running conditions on heat release in a Diesel engine. Also, Galindo et al. [12] used four different Weibe functions to account for pilot injection, premixed, diffusion, and late combustion in the heat release model. Chemla et al. [13] used a zero-dimensional rate of heat release model for the simulation of direct injection Diesel engine.

The objective of the present work is to analyze the performance of a CI engine using a computational thermodynamic model, similar to the one developed previously by the authors for the simulation of SI engines. This new developed model predicts in-cylinder temperatures and pressures as functions of the crank angle, with the application of a dual Weibe function for the heat release pattern. It also takes into consideration the effects of heat losses and temperature-dependent specific heats. These features can be very useful in providing more realistic estimations of the main performance parameters, such as the thermal efficiency and the break mean effective pressure, in comparison with the existing models for CI engines.

2. Thermodynamic analysis

For a closed system, the first law of thermodynamics is written as:

$$\delta Q - \delta W = dU \quad (1)$$

Abbreviations: BDC, Bottom dead center; TDC, Top dead center.

[☆] Communicated by W.J. Minkowycz.

* Corresponding author. Leibniz Universität Hannover, Intitute für Technishe Verbrennung, Welfengarten 1a, 30167 Hannover, Germany.

E-mail address: eiyad@hu.edu.jo (E. Abu-Nada).

Nomenclature

a	Constant used in Eq. (18)
A	Heat transfer area, m^2
AF	Air–fuel ratio, dimensionless
AF_s	Air–fuel ratio for stoichiometric condition, dimensionless
a_s	Number of moles of air at stoichiometric condition, dimensionless
BMEP	Brake mean effective pressure, bar
C_p	Constant pressure specific heat, $kJ/kg\ K$
C_1	Constant used in Eq. (16)
C_v	Constant volume specific heat, $kJ/kg\ K$
D	Cylinder diameter, m
h	Heat transfer coefficient for gases in the cylinder, W/m^2K
k	Specific heat ratio, dimensionless
LHV	Lower heating value, kJ/kg
l	Connecting rod length, m
m	Mass of cylinder contents, kg
m_f	Mass of fuel in the cylinder, kg
m_d	Constant used in Eq. (18)
m_p	Constant used in Eq. (18)
M	Molar mass
N	Engine speed, rpm
p	Pressure inside cylinder, bar
p_i	Inlet pressure, bar
p_r	Reference state pressure
Q	Heat transfer, kJ
Q_{in}	Heat added from burning fuel, kJ
Q_d	Integrated energy release for diffusion combustion phases, kJ
Q_{loss}	Heat losses, kJ
Q_p	Integrated energy release for premixed combustion phases, kJ
R	Crank radius, m
R_g	Gas constant, $kJ/kg\ K$
S	Engine stroke, m
T_g	Gas temperature in the cylinder, K
T_{gr}	Reference state gas temperature, K
T_i	Inlet temperature, K
T_w	Cylinder temperature, K
U	Internal energy, kJ
U_p	Piston speed, m/s
V	Cylinder volume, m^3
V_c	Clearance volume, m^3
V_d	Displacement volume, m^3
V_r	Reference state volume, m^3
X	Distance from top dead center, m
w	Average cylinder gas velocity, m/s
W	Work, kJ
θ	Crank angle, degree
θ_d	Duration of the diffusion combustion phases, degree
θ_p	Duration of the premixed combustion phases, degree
$\Delta\theta$	Duration of combustion, degree
ϕ	Equivalence ratio

By using the definition of work, the first law can be expressed as:

$$\delta Q_{in} - \delta Q_{loss} - (pdV) = dU \quad (2)$$

For an ideal gas the equation of state is expressed as:

$$pV = mR_g T_g \quad (3)$$

By differentiating Eq. (3), the following equation is obtained:

$$pdV + Vdp = mR_g dT_g \quad (4)$$

Also, for an ideal gas the change in internal energy is expressed as:

$$dU = d(mC_v T_g) \quad (5)$$

Using the chain rule of differentiation, Eq. (5) is rearranged as:

$$mR_g T_g = \frac{R_g}{C_v} (dU - mT_g dC_v) \quad (6)$$

By substituting Eq. (6) into Eq. (4) and solving for the change in internal energy:

$$dU = \frac{C_v}{R_g} (pdV + Vdp) + mT_g dC_v \quad (7)$$

Also, by substituting Eq. (7) into Eq. (1), the first law is written as:

$$\delta Q_{in} - \delta Q_{loss} - pdV = \frac{C_v}{R_g} (pdV + Vdp) + mT_g dC_v \quad (8)$$

Dividing Eq. (8) by $d\theta$

$$\frac{\delta Q_{in}}{d\theta} - \frac{\delta Q_{loss}}{d\theta} - p \frac{dV}{d\theta} = \frac{C_v}{R_g} \left(p \frac{dV}{d\theta} + V \frac{dp}{d\theta} \right) + mT_g \frac{dC_v}{d\theta} \quad (9)$$

Expressing the gradient of the specific heat as:

$$\frac{dC_v}{d\theta} = \frac{dC_v dk}{dk d\theta} \quad (10)$$

Noting that:

$$\frac{R_g}{C_v} = k - 1 \quad (11)$$

Plugging Eq. (11) into Eq. (10), then the gradient of the specific heat is expressed as:

$$\frac{dC_v}{d\theta} = - \frac{R_g}{(k-1)^2} \frac{dk}{d\theta} \quad (12)$$

Substituting Eq. (12) into Eq. (9), the final form of the governing equations is:

$$\frac{dp}{d\theta} = \frac{k-1}{V} \left(\frac{dQ_{in}}{d\theta} - \frac{dQ_{loss}}{d\theta} \right) - k \frac{p}{V} \frac{dV}{d\theta} + \frac{p}{k-1} \frac{dk}{d\theta} \quad (13)$$

In Eq. (13), the rate of the heat loss $\frac{dQ_{loss}}{d\theta}$ is expressed as:

$$\frac{dQ_{loss}}{d\theta} = hA(\theta)(T_g - T_w) \left(\frac{1}{\omega} \right) \quad (14)$$

The convective heat transfer coefficient is given by the Woschni model as [10,15,16]:

$$h = 3.26D^{-0.2} p^{0.8} T_g^{-0.55} w^{0.8} \quad (15)$$

The velocity of the burned gas and is given as:

$$w(\theta) = 2.28 \bar{U}_p + C_1 \frac{V_d T_{gr}}{p_r V_r} (p(\theta) - p_m) \quad (16)$$

The quantities V_r , T_{gr} , and p_r are reference state properties at closing of inlet valve and p_m is the pressure at same position to obtain

p without combustion (pressure values in cranking). Engine and operational specifications used in present simulation are given in Table 1. The value of C_1 is given as: for compression process: $C_1 = 0$ and for combustion and expansion processes: $C_1 = 0.00324$. The average piston speed \bar{U}_p is calculated from:

$$\bar{U}_p = \frac{2NS}{60} \quad (17)$$

On the other hand, the rate of the heat input $\frac{dQ_{in}}{d\theta}$ (heat release) can be modeled using a dual Weibe function [9,10]:

$$\frac{dQ_{in}}{d\theta} = a \left(\frac{Q_p}{\theta_p} \right) m_p \left(\frac{\theta}{\theta_p} \right)^{m_p-1} \exp \left(-a \left(\frac{\theta}{\theta_p} \right)^{m_p} \right) + a \left(\frac{Q_d}{\theta_d} \right) m_d \left(\frac{\theta}{\theta_d} \right)^{m_d-1} \exp \left(-a \left(\frac{\theta}{\theta_d} \right)^{m_d} \right) \quad (18)$$

where p and d refer to premixed and diffusion phases of combustion. The parameters θ_p and θ_d represent the duration of the premixed and diffusion combustion phases. Also, Q_p and Q_d represent the integrated energy release for premixed and diffusion phases respectively. The constants a , m_p , m_d are selected to match experimental data. For the current study, these values are selected as 6.9, 4, and 1.5 respectively [9,10]. It is assumed that the total heat input to the cylinder by combustion for one cycle is:

$$Q_{in} = m_f LHV \quad (19)$$

where 20% of this amount is assumed to take place in the premixed phase and the rest in the diffusion phase. Fig. 1 shows a plot for the rate of heat addition as a function of crank angle.

Eq. (13) is discretized using a second order finite difference method to solve for the pressure at each crank angle (θ) [1–4]. Once the pressure is calculated, the temperature of the gases in the cylinder can be calculated using the equation of state as:

$$T_g = \frac{p(\theta)V(\theta)}{mR_g} \quad (20)$$

The instantaneous cylinder volume, area, and displacement are given as [14]:

$$V(\theta) = V_c + \frac{\pi D^2}{4} x(\theta) \quad (21)$$

$$A_h(\theta) = \frac{\pi D^2}{4} + \frac{\pi DS}{2} (R + 1 - \cos(\theta) + (R^2 - \sin^2(\theta))^{1/2}) \quad (22)$$

$$x(\theta) = (\lambda + R) - (R \cos(\theta) + (\lambda^2 - \sin^2(\theta))^{1/2}) \quad (23)$$

Table 1
Engine and operational specifications used in simulation.

Fuel	C _{14.4} H _{24.9}
Compression ratio	18.
Cylinder bore (m)	0.105
Stroke (m)	0.125
Connecting rod length (m)	0.1
Number of cylinders	1
Clearance volume (m ³)	6.367 × 10 ⁻⁵
Swept volume (m ³)	1.082 × 10 ⁻³
Engine speed (rpm)	1000–5000
Inlet pressure (bar)	1
Equivalence ratio	0.2–1.2
Injection timing	–24° to –8°
Duration of combustion	60°
Duration of premixed combustion	8°
Wall temperature (K)	400

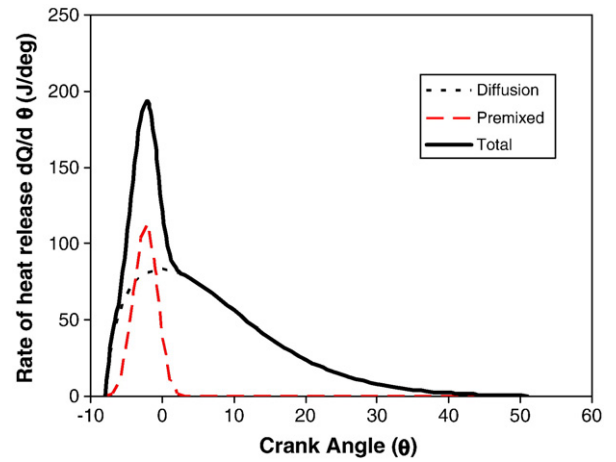


Fig. 1. Rate of heat release model $N = 2500$ rpm, $\Phi = 0.6$, $\theta_p = 10^\circ$ and $\theta_d = 60^\circ$ and injection is -8° .

An equation describing the variation of air specific heats for the temperature range 300–3500 K is adopted [17]. The equation is based on the assumption that air is an ideal gas mixture containing 78.1% N₂, 20.95% O₂, 0.92% Ar, and 0.03% Co₂ (on mole basis):

$$C_p = 2.506 \times 10^{-11} T_g^2 + 1.454 \times 10^{-7} T_g^{1.5} - 4.246 \times 10^{-7} T_g + 3.162 \times 10^{-5} T_g^{0.5} + 1.3303 - 1.512 \times 10^4 T_g^{-1.5} + 3.063 \times 10^5 T_g^{-2} - 2.212 \times 10^7 T_g^{-3} \quad (24)$$

It is found from Eq. (24) that specific heat at constant pressure increases with temperature from about 1.0 kJ/kg K at 300 K to about 1.3 kJ/kg K at 3000 K and such difference should be taken into consideration. Similarly, the specific heat ratio, k , decreases from 1.40 to about 1.28 within the same temperature range.

The thermal efficiency and the mean effective pressure are defined respectively as:

$$\eta = \frac{W_{net}}{Q_{in}} \quad (25)$$

$$BMEP = \frac{W_{net}}{V_d} \quad (26)$$

3. Results and discussion

A rate of heat release model for a Diesel engine, taking into consideration the heat transfer in the engine and variable specific heats of the air, using a dual Weibe function is presented in Fig. 1. Three combustion phases are observed, namely premixed combustion phase, diffusion combustion phase and late combustion phase.

Fig. 2 represents cylinder pressure versus volume for the Diesel engine running at 2500 rpm and $\Phi = 0.6$. The cylinder pressure reaches high values, around 90 bar. This value is considered high compared to SI engines because of the high compression ratio used in the Diesel engine. One of the most important factors affecting the performance of Diesel engines is the instant when combustion starts, which is controlled by the injection timing. In order to examine the effect of variation the injection timing Fig. 3 is presented. The figure shows the sensitivity of the pressure and temperature to the injection timing where the curves vary significantly. As shown from Fig. 3(a), early injection timing leads to high levels of pressure in the cylinder. For early injection most of combustion is taking place while the piston is moving toward the TDC. Therefore, the pressure increase is due to

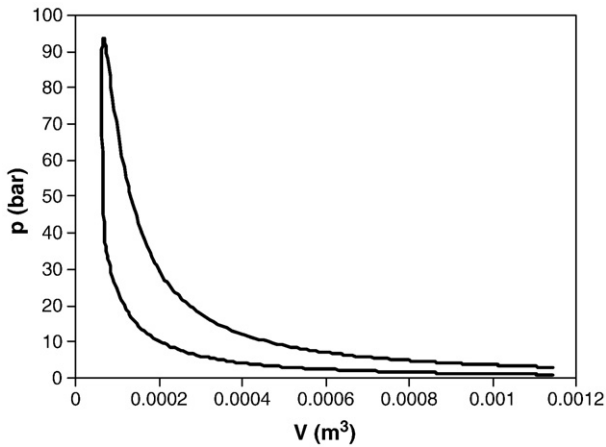


Fig. 2. Variation of cylinder pressure versus volume for Diesel engine running at 2500 rpm at $\phi = 0.6$.

twofold effect namely the compression of gases, due to movement of the piston, and the heat release during to combustion. This explains the higher level of pressure encountered in early injection timing. Also, Fig. 3(b) shows the effect of injection timing on the cylinder gases temperatures where a similar trend is observed. However, an interesting observation is that for $\theta > 20$ after the TDC, the gas temperature in the cylinder is highest for late injection timing. For $\theta > 20$, the heat addition in early injection, -24° , is almost in its last stages. However, for late injection timing of -8° , most of the heat release is still not supplied to the cylinder. Therefore, the heat release continues to take place for $\theta > 20$.

Fig. 4 present the variation of the outlet gas temperature and the maximum gas temperature versus engine speed. It is clear that the gas temperature increases with engine speed. The rate of increase in gas temperature is higher at low engine speed, below 200 rpm, than at

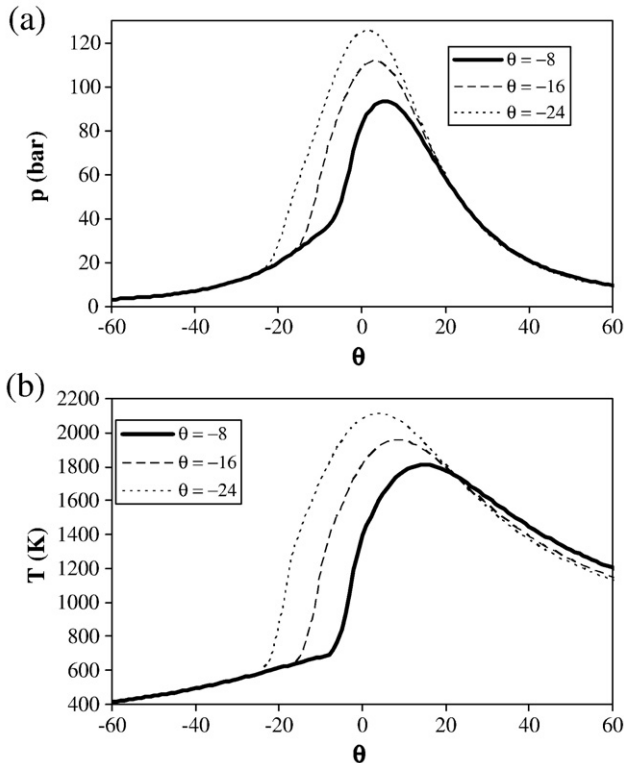


Fig. 3. Effect of variation of injection timing, $N = 2500$ rpm and $\phi = 0.6$ (a) Variation of cylinder pressure versus crank angle (b) Variation of gas temperature versus crank.

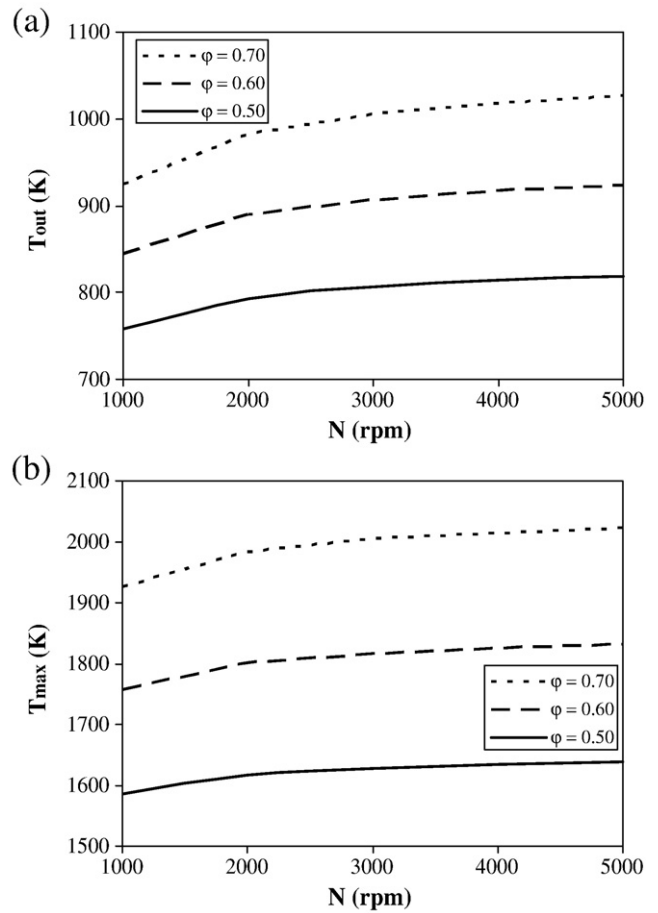


Fig. 4. Gas temperature versus engine speed at various equivalence ratios (a) Outlet temperature (b) Maximum temperature.

high engine speed. Also, the gas temperature increases with increasing the equivalence ratio. For higher equivalence ratio more fuel is burned in the cylinder and therefore more heat is released that leads to higher gas temperatures. It can be also observed that the effect of equivalent ratio is dominant over that of the engine speed.

Fig. 5 shows the BMEP variation with engine speed using different equivalence ratios. The BMEP increases with engine speed and equivalence ratio. However, BMEP is more sensitive to equivalence ratio than to engine speed. It is desirable from BMEP consideration to have high equivalence ratio to achieve high values of BMEP. However,

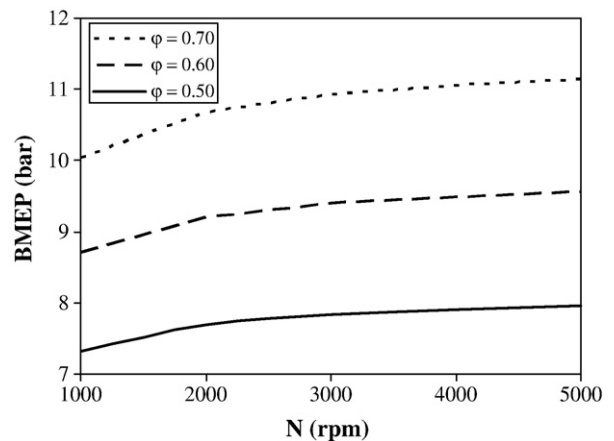


Fig. 5. Brake mean effective pressure versus engine speed at various equivalence ratios.

higher equivalence ratio has adverse effect on the thermal efficiency where values greater than unity corresponds to lower levels of thermal efficiency as demonstrated in Fig. 6.

Fig. 6 shows the optimum range of equivalence ratio is between 0.5 and 0.7 for engine speed between 2000 and 3000. However, for low engine speed, e.g., $N = 1000$, the optimum equivalence ratio is around 0.35. For low engine speed the thermal efficiency decreases by increasing equivalence ratio. Therefore, the increase in heat addition due to high values of Φ is countered by an excessive heat loss from the

cylinder due to the higher temperatures in the cylinder. For higher engine speed, this heat loss is still taking place; but, high engine speed leads to lower rates of heat loss as demonstrated by Eq. (14). Fig. 6(a) and (c) show that with higher engine speed and $0.5 < \Phi < 0.7$ the thermal efficiency reaches a value around 45%. Fig. 6(b) shows that higher engine speed leads to increase in thermal efficiency. Besides, for high engine speeds the efficiency becomes independent of the equivalence ratio.

4. Conclusion

Early injection timing leads to higher levels of pressure and temperature in the cylinder. It is found that BMEP is more sensitive to equivalence ratio than to engine speed. Higher values of equivalence ratio lead to lower thermal efficiency. For medium engine speed between 2000 and 3000 it is found that the optimum equivalence ratio is between 0.5 and 0.7. However, for low engine speed the optimum equivalence ratio is around 0.35. For high engine speeds the thermal efficiency is almost independent of equivalence ratio for $\Phi > 0.4$.

Acknowledgment

The corresponding author would like to thank the Alexander von Humboldt Foundation (AvH) for supporting his research stay at the Leibniz Universität Hannover.

References

- [1] E. Abu-Nada, I. Al-Hinti, A. Al-Sarkhi, B. Akash, Thermodynamic modeling of spark-ignition engine: effect of temperature dependent specific heats, International Communications in Heat and Mass Transfer 33 (10) (2006) 1264–1272.
- [2] E. Abu-Nada, I. Al-Hinti, B. Akash, Al-Sarkhi, Thermodynamic analysis of spark-ignition engine using a gas mixture model for the working fluid, International Journal of Energy Research 31 (2007) 1031–1046.
- [3] E. Abu-Nada, I. Al-Hinti, A. Al-Sarkhi, B. Akash, Effect of piston friction on the performance of SI engine: a new thermodynamic approach, ASME Journal of Engineering for Gas Turbines and Power 130 (2) (2008) 022802-1.
- [4] E. Abu-Nada, B. Akash, I. Al-Hinti, A. Al-Sarkhi, Performance of spark ignition engine under effect of friction using gas mixture model, Journal of the Energy Institute 82 (4) (2009) 197–205.
- [5] L. Chen, C. Wu, F. Sun, S. Cao, Heat transfer effects on the net work output and efficiency characteristics for an air-standard Otto cycle, Energy Conversion and Management 39 (1998) 643–648.
- [6] A. Parlak, Comparative performance analysis of irreversible Dual and Diesel cycles under maximum power conditions, Energy Conversion and Management 46 (3) (2005) 351–359.
- [7] S. Hou, Heat transfer effects on the performance of an air standard Dual cycle, Energy Conversion and Management 45 (2004) 3003–3015.
- [8] O. Ozsoysal, Heat loss as a percentage of fuel's energy in air standard Otto and Diesel cycles, Energy Conversion and Management 47 (2006) 1051–1062.
- [9] N. Miyamoto, T. Chikahisa, T. Murayama, R. Sawyer, Description and analysis of diesel engine rate of combustion and performance using Weibe's functions, SAE paper 850107, 1985.
- [10] C. Ferguson, A. Kirkpatrick, Internal Combustion Engines: Applied Thermosciences, Wiley, New York, 2001.
- [11] J. Arrègle, J.M. Garcia, J.J. Lopez, C. Fenollosa, Development of a zero-dimensional Diesel combustion model. Part 1: analysis of the quasi-steady diffusion combustion phase, Applied Thermal Engineering 23 (2003) 1301–1317.
- [12] J. Galindo, J.M. Lujan, J.R. Serano, L. Hernandez, Combustion simulation of turbocharger HSDI Diesel engines during transient operation using neural networks, Applied Thermal Engineering 25 (2005) 877–898.
- [13] F.G. Chemla, G.H. Pirkker, A. Wimmer, Zero-dimensional ROHR simulation for DI diesel engines – a generic approach, Energy Conversion and Management 48 (2007) 2942–2950.
- [14] W. Pulkrabek, Engineering fundamentals of the internal combustion engine, second ed. Pearson Prentice-Hall, Upper Saddle River, New Jersey, USA, 2004.
- [15] R. Stone, Introduction to internal combustion engines, 3rd ed. Palgrave, New York, 1999.
- [16] G. Woschni, Internationally applicable equation for the instantaneous heat transfer coefficient in internal combustion engine, SAE Paper no. 670931, 1967.
- [17] R. Sonntag, C. Borgnakke, G. Van Wylen, Fundamentals of thermodynamics, 5th ed. Wiley, New York, 1998.

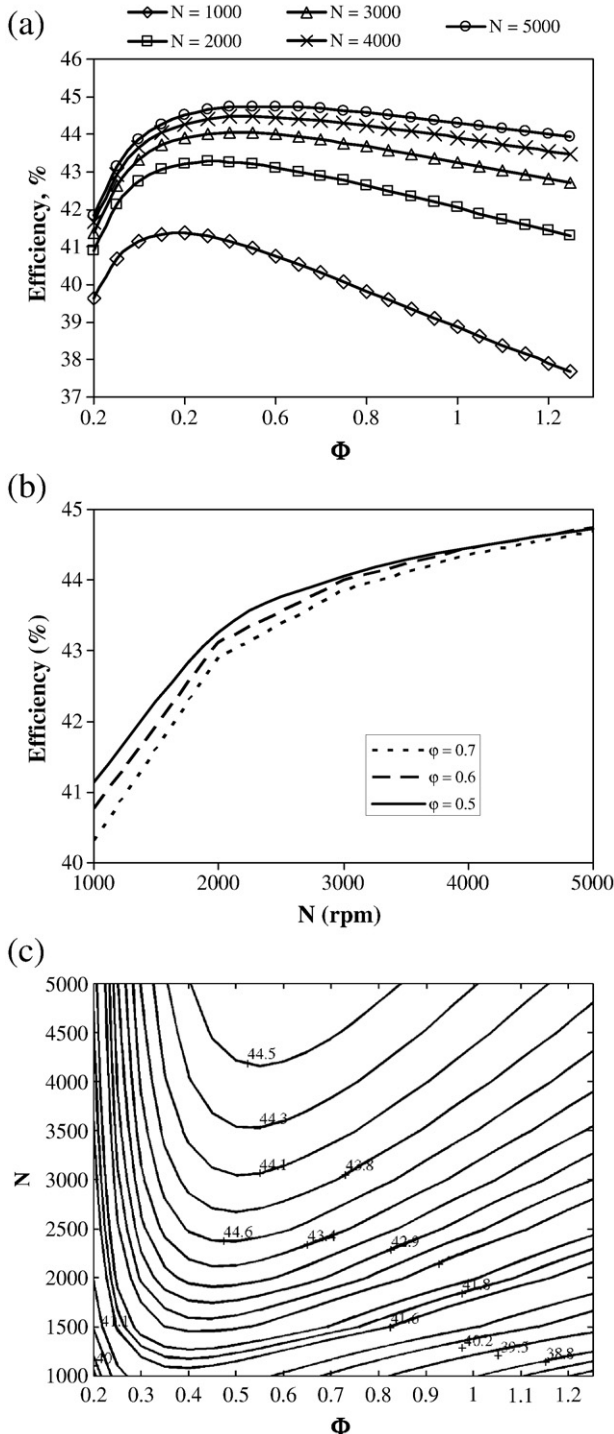


Fig. 6. Engine efficiency (a) Efficiency versus equivalence ratio (b) Efficiency versus engine speed (c) Efficiency contour plots.